Reversing an S-kink effect caused by interface degradation in organic solar cells through gold ion implantation in the PEDOT:PSS layer

D. Brenes-Badilla, D. J. Coutinho, D. R. B. Amorim, R. M. Faria, and M. C. Salvadori

---

Articles you may be interested in

Accurate reconstruction of the jV-characteristic of organic solar cells from measurements of the external quantum efficiency
Journal of Applied Physics **123**, 134501 (2018); 10.1063/1.5009155

On the front and back side quantum efficiency differences in semi-transparent organic solar cells and photodiodes
Journal of Applied Physics **123**, 125501 (2018); 10.1063/1.5017030

Carrier-selective interlayer materials for silicon solar cell contacts
Journal of Applied Physics **123**, 143101 (2018); 10.1063/1.5020056

Abnormal staircase-like I-V curve in InGaN quantum well solar cells
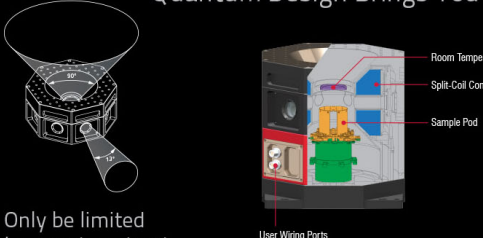Applied Physics Letters **112**, 161102 (2018); 10.1063/1.5018481

Accessing the band alignment in high efficiency $Cu(In,Ga)(Se,S)_2$ (CIGSSe) solar cells with an In_xS_y:Na buffer based on temperature dependent measurements and simulations
Journal of Applied Physics **123**, 155701 (2018); 10.1063/1.5017087

Negative differential resistance in nickel octabutoxy phthalocyanine and nickel octabutoxy phthalocyanine/graphene oxide ultrathin films
Journal of Applied Physics **123**, 155501 (2018); 10.1063/1.5021719

Reversing an S-kink effect caused by interface degradation in organic solar cells through gold ion implantation in the PEDOT:PSS layer

D. Brenes-Badilla,[1] D. J. Coutinho,[2,3] D. R. B. Amorim,[2] R. M. Faria,[2] and M. C. Salvadori[1,a)]

[1]*Instituto de Física, Laboratório de Filmes Finos – Universidade de São Paulo, Brazil*
[2]*Departamento de Física e Ciência dos Materiais, Instituto de Física de São Carlos, Universidade de São Paulo, Brazil*
[3]*Federal Technological University of Paraná (UTFPR), Toledo, PR, Brazil*

In this work, we performed a study on the recovery of the photovoltaic performance of an ITO/PEDOT:PSS/P3HT:PCBM/Ca/Al solar cell after the hole transport layer (PEDOT:PSS) had been degraded by contact with the environment. A device that was fully built in an inert environment exhibited a fill factor (*FF*) of 0.64, while the device whose hole transport layer was exposed to air presented a *FF* equal to 0.2. In addition, the *J-V* characteristic curve of the degraded device did not follow the photovoltaic pattern exhibiting the degenerate S shape. However, the elimination of the deleterious effect was achieved by bombarding gold ions on the contaminated surface of PEDOT:PSS by means of the Metal Plasma Immersion Ion Implantation technique. Due to the low energy of the ionic beam of gold, the implanted gold atoms were located at few nanometers off the surface, forming nanometric clusters, that is, gold nanoparticles. Most probably, the degradation of the *J-V* photovoltaic curve, represented by the S-kink effect, was caused by the appearance of a potential barrier at PEDOT:PSS/P3HT:PCBM interface, which was demolished by the gold nanoparticles that have work function close to HOMO of P3HT. This S-kink effect was also simulated by using an equivalent circuit model constituted by a two-diode circuit, one of which plays the role of the undesirable potential barrier formed at the PEDOT:PSS/P3HT:PCBM interface. Our analysis shows that deposition of gold nanoparticles next to the interface recovers the good hole injection condition from the PEDOT:PSS into the active layer, restoring the fill factor and the device efficiency. *Published by AIP Publishing.* https://doi.org/10.1063/1.5017672

INTRODUCTION

Bulk Heterojunction Organic Solar Cells (BHJ-OSCs) have been the subject of extensive research over the past few years, as they show great potential to become a commercially available technology for renewable energy production.[1–4] Flexibility, lightness, processability in solution, and inexpensive manufacturing are some of the desired features that have stimulated the technology of BHJ-OSCs.[5,6] The two-phase morphology of the active layer in BHJ-OSCs, which is composed of a nanometric mixture of an electronic polymer, as donor, and a certain acceptor molecule, allows a complete conversion of photogenerated excitons into charge carrier pairs. In such a configuration, a BHJ-OSC has exhibited a power conversion efficiency (PCE) above 10%.[7–10] However, the BHJ-OSC technology is still far from penetrating the energy conversion market because many drawbacks need to be overcome, for example, noxious effects at interfaces of successive internal layers. The search for improvement of stability and increased operating lifetime of BHJ-OSCs has been requesting a great effort of research on organic photovoltaics.[11,12] Thereby, the performance of a solar cell depends not only on the properties of the donor–acceptor absorbing layer, but also on the properties of interfaces between the multilayer components.[13] One of the most common undesired effects in the BHJ-OSCs is the

arising of S-kink in the current density-voltage (*J-V*) curve of the cell under illumination, which deteriorates the shunt and the series resistances, reducing significantly their fill factor (FF) and its power conversion efficiency (PCE).[14–21] Several explanations have been proposed for the S-kink effect: interfacial dipole formation,[5] charge accumulation,[6,7] contact degradation effects,[3,7,16,22,23] imbalance in the electron and hole mobility,[6,17] reduction in the charge carrier extraction,[7,18] and phase separation of the two organic components.[19] It has also been shown that degradation of the hole transport layer (HTL) is responsible for many effects that degenerate the *J-V* photovoltaic curve. Street *et al.* showed that the degradation of BHJ-OSCs resulting from ambient exposure affects preferentially the hole transport layer instead of the active layer,[24] while Wagner *et al.* demonstrated that increasing the value of the work function of HTL reduces eventual potential barriers between the Fermi level of the anode and the HOMO level of the active layer, thereby decreasing the series resistance of the interfaces and increasing the fill factor of the device.[19] By investigating the degradation effects in indium-tin oxide (ITO)/TiO$_2$/P3HT:PCBM/MoO$_3$/Ag inverted solar cells, Sundqvist *et al.* showed that a robust S-kink was removed by exposing the cell to UV light (light-soaking). In this work, the authors concluded that the improved performance was obtained by the decrease in the work function of ITO/TiO$_2$.[25] In addition, simulations of *J-V* photovoltaic curve of a BHJ-OSC, carried out by Yang and collaborators,

a)Author to whom correspondence should be addressed: mcsalvadori@if.usp.br

showed that S-kink arises when the hole injection barrier exceeds 0.2 eV, which is most probably due to accumulated charge carriers at the vicinity of the contact.[26] Nevertheless, further experimental investigations are still necessary to shed light on the origin of the S-kink phenomenon and mainly to provide methods to consistently eliminate it.

In this work, we show that an S-kink effect in an ITO/PEDOT:PSS (poly(3,4-ethylenedioxythiophene)-poly(styrenesulfonate))/rr-P3HT:PCBM/Ca/Al device arises due to the exposition of PEDOT:PSS layer to air. However, this deleterious effect is largely reduced when gold nanoparticles (AuNPs) are implanted at a few nanometers from the degraded surface of PEDOT:PSS, recovering the good performance of the solar cell, despite eventual undesirable effects of absorption or reflection by gold particles.[27]

This study was made by comparing three identical devices, manufactured side by side on the same substrate, except that, in two of them, the PEDOT:PSS layer was exposed to air, while the other was all the time protected from external contact, and used as reference. One of the devices that had the degraded PEDOT:PSS layer exhibited the S-Kink in the current-voltage curve under illumination. The second device had the degraded layer bombarded by ionic beam of gold, and the device manufactured with it showed a performance compared with the reference device. Based on equivalent circuit models, which had been recently described in the literature,[28,29] we analyzed the results of the degraded cell by making use of a two-diode equivalent circuit, in which the additional diode in the traditional equivalent circuit of a solar cell represents an energy barrier formed at the PEDOT:PSS/P3HT:PCBM interface. Therefore, the incorporated AuNPs at the hole transport layer had recovered the former interfacial properties, most probably restoring the electronic structure appropriate to the injection of holes that would have been damaged by the action of oxygen.

EXPERIMENTAL

We prepared two ITO/PEDOT:PSS/rr-P3HT:PCBM/Ca/Al devices on the same batch, side by side, obeying the procedure described as follows. First, a glass substrate with a patterned indium-tin oxide (ITO) was cleaned in an ultrasonic detergent bath (60 °C), then with acetone and isopropanol for 10 min each, and finally dried under nitrogen gas flow. The ITO surface was then treated for 10 min in the UV-ozone cleaning chamber to remove residual organic contaminants. PEDOT:PSS (Clevios P Al 4083) was spin-cast at 3000 rpm for one minute to form films of 35 nm thick, which were annealed at 120 °C for 10 min. After thermal annealing, the ITO/PEDOT:PSS films were exposed to air for a few days, to provoke reduction reaction or other degradation effects. Before finalizing the manufacture of the devices, in one of them, ion gold was implanted through the surface of PEDOT:PSS film. For this, we used the Plasma Immersion Ion Implantation &and Deposition (MEPIIID) technique with a very low ion energy implantation (49 eV), which provides a unidirectional flux of charge-neutral plasma.[30,31] The implantation dose was of 6.4×10^{15} ions/cm^2, measured through Rutherford backscattering spectrometry (RBS). During the gold ion implantation, the non-implanted device was protected by a metallic shadow mask [Fig. 1(a)]. Thereby, it resulted in one non-implanted ITO/PEDOT:PSS structure and other similar structure in which the layer of PEDOT:PSS was implanted with gold ions [Fig. 1(b)].

It has been observed that metal implantation above the solubility limit in a given substrate generates metal nanoparticles nucleation and growth.[32] In this way, gold ion implantation, using very low energy (49 eV), nucleate gold nanoparticles in the maximum gold concentration depths in the PEDOT:PSS film, generating an array of nanoparticles at approximately 3 nm depth,[33] as determined by the implantation profile [Fig. 2(a)] calculated by Monte Carlo simulation using the highly reliable TRIDYN software package.[34,35] Nevertheless, recent Transmission Electron Microscopy (TEM) images of cross-section of PMMA bombarded by gold under the same conditions showed that after implantation, the diffusion mechanism extend the penetration up to a depth of 10 nm. Field Emission Scanning Electron Microscopy (FE-SEM) images of the implanted PEDOT:PSS surface show the formation of AuNPs having average diameters not higher than 10 nm [Fig. 2(b)]. It is important to stress that, most probably, the AuNPs are not spheroids, but probably flattened nanospheres. Figure 2(c) shows similar FE-SEM image obtained in a non-implanted region for terms of comparison. These images were performed with an INSPECT F50 Field Emission Gun (FEG)–SEM microscope.
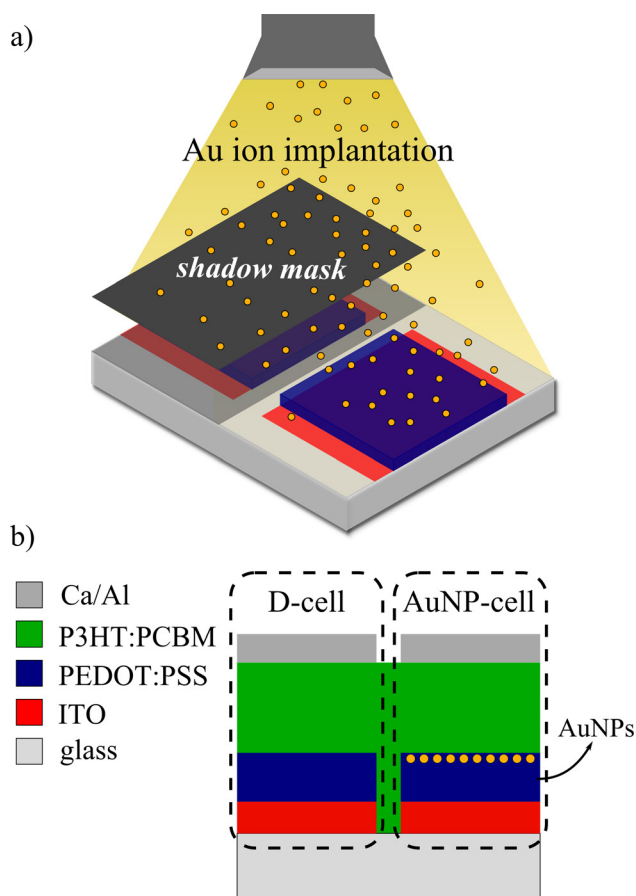

FIG. 1. (a) Au ion implantation on PEDOT:PSS layer by the Metal Plasma Immersion Ion Implantation and Deposition (MEPIIID) technique; (b) final device structure ITO/PEDOT:PSS/rr-P3HT:PCBM/Ca/Al of D-cell and AuNP-cell built on the same substrate.
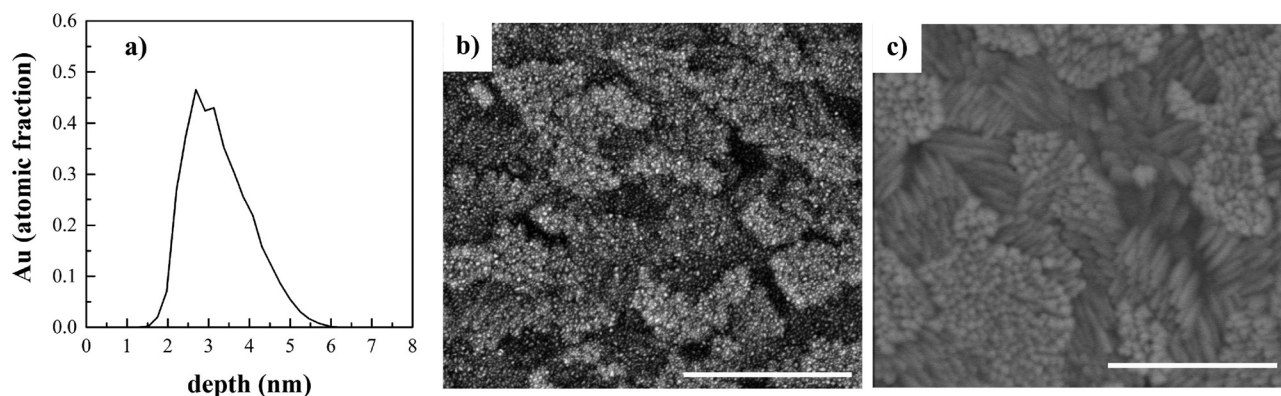
FIG. 2. (a) Depth profile of Au implanted PEDOT:PSS for the ion energy (49 eV) and dose (6.4×10^{15} ions/cm^2) used in this experiment, as calculated by the TRIDYN simulation code; (b) FE-SEM micrograph of a PEDOT:PSS thin film containing the AuNPs: the white bar represents 400 nm length; (c) FE-SEM micrograph of a neat PEDOT:PSS thin film over ITO substrate: the white bar represents 400 nm length.

The manufacture of both devices was then completed inside a glovebox, filled with nitrogen, where the active layer was deposited using a ready-to-use electronic ink (purchased from Aldrich) consisting of rr-P3HT:PCBM mixture dissolved in 1,2-dichlorobenzene. The ink was spin-cast at 1000 rpm for 3 min resulting in a 170 nm-thick film. Thermal annealing was performed on a hot plate at 140 °C for 10 min. Finally, a top electrode made of calcium (30 nm) and aluminum (70 nm) was thermally evaporated through a shadow mask under low pressure (10^{-6} mbar). The ITO/PEDOT-PSS/rr-P3HT:PCBM/Ca/Al devices were then distinguished by the PEDOT:PSS layer characteristics, i.e., one being degraded by air exposition, which was nominated by D-cell, and the other in which gold was implanted in the degraded PEDOT:PSS, identified as AuNP-cell [Fig. 1(b)]. As a comparison guide, a third device of the same architecture was built entirely within the glovebox, and referred to as the reference cell (R-cell).

Kelvin Probe Force Microscopy (KPFM) technique (NanoScope IIIA-Bruker) was used to measure the temporal evolution of the contact potential difference (V_{CPD}) of a neat PEDOT:PSS during its exposition to air. Finally, current density-voltage (J-V) curves were measured with a Keithley 2400 source measurement unit, and the device was illuminated with an Oriel Sol3A Class AAA Solar Simulator, which gives the AM 1.5 G (100 mW/cm^2) condition. All J-V curves were measured under N$_2$ atmosphere and at room temperature.

RESULTS AND DISCUSSION

The J-V curves displayed in Fig. 3(a), from D-cell and AuNP-cell, shows how efficient the implantation of gold was in the recovering of a good performance of the solar cell. There was a considerable improvement in the values of the series resistance (R_s), the parallel resistance (R_{sh}), and the fill factor (FF). The comparison of the current density vs voltage (J-V) measurements obtained in the D-cell and AuNP-cell devices, under AM 1.5 G ($I_0 = 100$ mW/cm^2) condition, shows that the unsatisfactory values of the series (R_s) and shunt resistances (R_{sh}) as well as those of the fill factor (FF) shown in the D-cell are greatly improved in the AuNP-cell
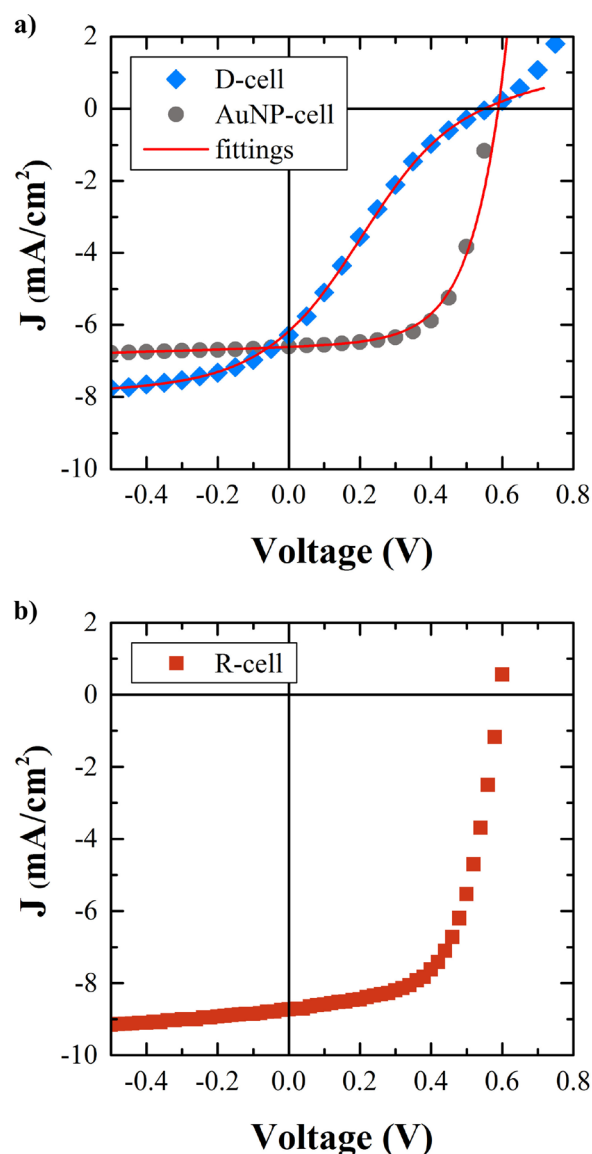

FIG. 3. (a) J-V characteristics of degraded and Au-implanted solar cells characterized under AM 1.5 illumination (100 mW/cm^2). In red is shown the fit using the modified circuit model given by Eq. (1) (D-cell) and Eq. (2) (AuNP-cell). (b) J-V curve under illumination of Reference cell.

[Fig. 3(a)]. That is, while the shape of the J-V curve of the D-cell shows the deleterious effect of the S-kink effect, the response of the AuNP-cell recovered the shape of the reference R-cell [Fig. 3(b)]. This result indicates that the degradation caused by the air exposure of the PEDOT:PSS was responsible for the appearance of the S-kink effect, and that the formation of gold nanoparticles just below the PEDOT:PSS surface, by the ion implantation technique, somehow eliminated the negative effect of exposure to air. Table I displays the values extracted from Fig. 3 for the short-circuit currents (J_{sc}), the open circuit voltages (V_{oc}), the fill factors (FF), the power conversion efficiencies (PCE), and the series and shunt resistances (R_s and R_{sh}), of the three cells: D-cell, AuNP-cell, and R-cell. The values of FF, PCE, and resistances R_s and R_{sh} obtained from D-cell device were 20%, 0.7%, 196 Ω cm^2, and 110 Ω cm^2, respectively. Much better values were obtained in AuNP-cell: $FF = 64\%$, $PCE = 2.36\%$, $R_s = 14$ Ω cm^2, and $R_{sh} = 1815$ Ω cm^2. Therefore, the similarity between the J-V curves of the AuNP-cell and R-cell, and the values of the characteristic parameters of the solar cells, confirm that the ion implantation in the PEDOT:PSS layer destroyed the deleterious effects caused by its exposure to the environment.

As already mentioned in the introduction, the literature is rich in results that indicate that the degradations of materials that compose the electrodes and/or the charge carriers transport layers are factors that generate S-kinks in photovoltaic J-V curves, and hence cause damage on the device performance. Jin et al. showed that the thermal degradation of PEDOT:PSS causes a decrease in the fill factor and the appearance of the S-kink in the photovoltaic curve of a P3HT:PCBM solar cell.[36] Other investigations concluded that charge carrier accumulation at the vicinity of the active layer is the origin of this S-kink effect, which would generate an interfacial electric field reducing the effective potential along the active layer.[37] Based on the solvent effect on the PEDOT:PSS layer, Namkoong et al. concluded that the weakening of the electric field inside the active layer of a P3HT:PCBM solar cell leads to the impoverishment of extraction charges, and consequently, the decrease in device efficiency.[38] They proposed that this effect is caused by the emergence of an energy barrier at the PEDOT:PSS/P3HT:PCBM interface caused by a decrease in the work function of PEDOT:PSS. Kumar and collaborators obtained similar results, i.e., the undesirable S-kink, by introducing an energy barrier caused by a layer of Bathocuprine (BCP) between the PEDOT:PSS and the active layer.[15] They attributed the appearance of the S-curve to a dipolar effect located at the BCP layer, and to explain this effect, they developed a drift-diffusion model that takes into account the effects of chemisorption at interfaces between intermediate layers and the active layer.

Similar conclusion were obtained by Street et al. in an experimental investigation[24] and by Yang et al.,[26] who simulated the influence of the injection barrier on the performance of organic solar cells, including the influence on the S-kink curve. More recently, Gusain et al. using Kelvin Probe and XPS analysis showed that work function of PEDOT:PSS can vary up to 0.2 V due to chemisorbed oxygen (O_2^-). In this case, oxygen molecules would modify the PEDOT:PSS/PCDTBT:PCBM interface characteristic in a bulk heterojunction solar cell, resulting in the appearance of an S-kink.[39] In order to check the action of air on the electrical properties of PEDOT:PSS surface, we carried out a contact potential difference (V_{CPD}) measurement in a neat PEDOT:PSS layer exposed to air, by KPFM technique, and we observed that V_{CPD}, and therefore work function of PEDOT:PSS, experimented a variation of 0.2 V after few hours of air exposure (Fig. 4). This leads us to conclude that degradation caused by air exposition builds a barrier for hole injection into the active layer, in agreement with the hypothesis raised by the works above-mentioned.

To further explore the parameters of the D-cell, we resort to the equivalent circuit model proposed by Castro,[40] in which, in our case, a second diode represents the barrier effect caused by charge carrier accumulation at the interface (Fig. 5). Circuit 2 is the additional circuit containing a rectifying diode (J_{d2}) in parallel with a resistor R_{sh2}. An analytical expression for this circuit was derived by Romero et al., who made use of the Kirchoff's law and the Lambert W-function, whose equation gives the dependence of the voltage V in function of the measured density electric current J,[41]

$$V = (J + J_{ph} + J_{01})R_{sh1} - \frac{n_1 k_B T}{q} W$$
$$\times \left\{ \frac{q}{n_1 k_B T} J_{01} R_{sh1} \exp\left[\frac{q}{n_1 k_B T} R_{sh1}(J + J_{ph} + J_{01}) \right] \right\}$$
$$+ (J - J_{02})R_{sh2} + \frac{n_2 k_B T}{q} W$$
$$\times \left\{ \frac{q}{n_2 k_B T} J_{02} R_{sh2} \exp\left[\frac{-q}{n_2 k_B T} R_{sh2}(J - J_{02}) \right] \right\} + J R_s.$$

(1)

TABLE I. Summary of the D-cell, AuNP-cell, and R-cell device parameters. R_s and R_{sh} were obtained from slope^{-1} of J-V curve at $V = 0$ (R_{sh}) and $V = V_{OC}$ (R_s).

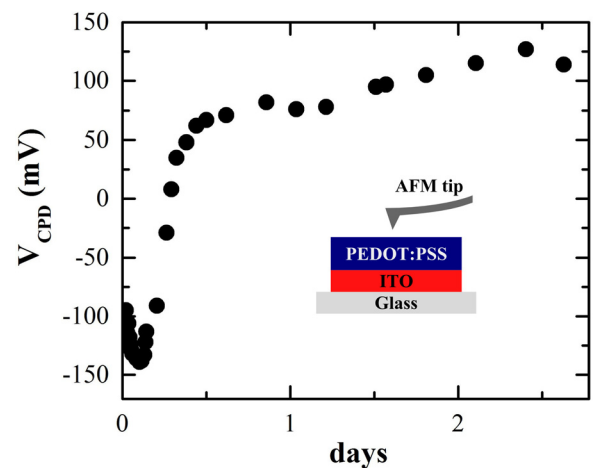|	J_{SC} (mA/cm^2)	V_{OC} (V)	FF (%)	PCE (%)	R_s (Ω cm^2)	R_{sh} (Ω cm^2)
D-cell	6.3	0.56	20	0.7	196	110
AuNP-cell	6.6	0.56	64	2.4	14	1815
R-cell	8.7	0.58	61	3.1	12	1000

FIG. 4. Contact potential difference of PEDOT:PSS layer measured at different exposition times to the environment.
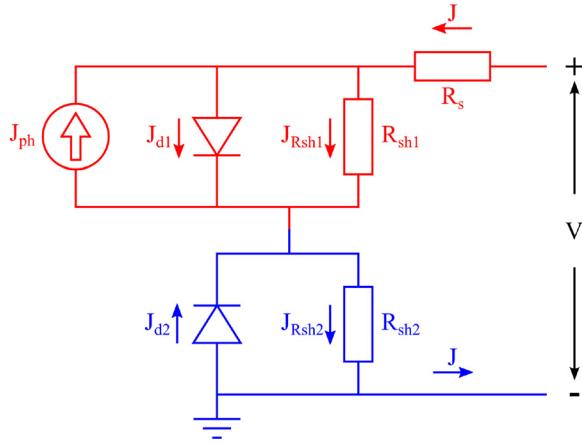
FIG. 5. Modified equivalent circuit proposed by Castro *et al.*[40] The red part is the traditional equivalent circuit (circuit 1) often used to parameterize organic solar cells, and in blue is shown the additional circuit (circuit 2) including a rectifying diode (diode 2) in parallel with a resistor R_{sh2}.

In this expression, J_{ph} is the saturated photocurrent, J_0 is the reverse saturation current in dark, n is the ideality factor, R_s is the series resistance, and R_{sh} is the shunt resistance. The indices 1 and 2 addressed to the equivalent circuit 1 and 2, which represent, respectively, the ITO/PEDOT:PSS and the P3HT:PCBP/Ca-Al parts of the degraded device. Equation (1) was then used to fit the *J-V* curve of the D-cell, whose result is the continuous red line shown in Fig. 3(a). The fitting for the AuNP-cell was performed by a traditional equation [Eq. (2)] of the equivalent circuit (circuit 1) of classical solar cells, i.e.,

$$J(V) = J_o \left\{ \exp\left[\frac{q(V - JR_s)}{nkT} \right] - 1 \right\} + \frac{V - JR_s}{R_{sh}} - J_{ph}. \quad (2)$$

A summary of the adjusted parameters obtained from Eq. (1) for the *J-V* curve of D-cell [Fig. 3(a)] is shown in Table II. The adjusted value for J_{ph} is coherent with those of J_{sc} recorded from the D-cell and the AuNP-cell. The same we can say for J_{01} and J_{02}, which are very small compared with J_{ph}. The model is also consistent for the adjusted values of the resistances of both cells, because the adjusted values of R_s (AuNP-cell) and R_{sh1} are equal to those shown in Table I. The measured value of the series resistance of D-cell (Table I) is close to the sum of the adjusted R_{sh2} with the series resistance R_s of the AuNP cell. The agreement among the parameters obtained from the experiments with those calculated by expressions (1) and (2) corroborates the hypothesis that a potential barrier was formed in the PEDOT:PSS/P3HT:PCBM interface due to exposition to air. In addition, the implantation of gold ions, which generated a layer of gold nanoparticles near the surface of the

PEDOT:PSS, seems to be the key factor that eliminated the adverse effect of this potential barrier, recovering then the good performance of the solar cell. As a final explanation, we can infer that the HOMO level of PEDOT (∼5.1 eV), which is close to the HOMO of P3HT (5.2 eV), had its value decreased by 0.2 eV due to degradative action of air as shown in Fig. 4. This effect can be the reason for the barrier formation for the injection of holes, leading to an S-kink in the *J-V* curve. The generated Au nanoparticles, which have work function around 5.4 eV,[42] thus restored the hole injection from the PEDOT:PSS layer into the P3HT:PCBM active layer.

CONCLUSIONS

In this paper, we show that degradation of the PEDOT:PSS layer by exposition to air causes a worsening in the performance of an ITO/PEDOT:PSS/rr-P3HT:PCBM/Ca/Al solar cell, mainly in the fill factor, in the series, and in shunt resistances, and consequently, in power conversion efficiency. It is known from the literature that charge carrier accumulation at interfaces between transport layers and the active layer creates an interfacial energy barrier. Through contact potential difference measurement, we were able to measure this barrier, which, among other effects, diminishes the effective electric field inside the active layer, degrades the properties of the multilayer solar cells, and results in the emergence of S-shape in the current-voltage (J-V) curve under illumination. We conclude that the degradation of PEDOT:PSS due to oxygen, in our case, is responsible for the S-kink recorded in the D-cell. This was supported by the extracted solar cell parameters using the equivalent circuit model proposed by Castro and collaborators [40] and analytically solved by Romero *et al.*[41] Finally, the deleterious effect caused by degraded PEDOT:PSS was substantially removed by incorporating gold nanoparticles in the PEDOT:PSS film close to the rr-P3HT:PCBM active layer.

TABLE II. Summary of the adjusted parameters of *J-V* curve of D-cell from Eq. (1).

R_s ($\Omega \cdot cm^2$)	J_{ph} (mA/cm^2)	J_{01} ($\mu A/cm^2$)	J_{02} ($\mu A/cm^2$)	n_1	n_2	R_{sh1} ($\Omega \cdot cm^2$)	R_{sh2} ($\Omega \cdot cm^2$)
14	7.6	146	1.43	5.61	1.0	1815	177

[1]D. J. Coutinho, G. C. Faria, D. T. Balogh, and R. M. Faria, Sol. Energy Mater. Sol. Cells **143**, 503 (2015).
[2]C. J. Brabec, S. Gowrisanker, J. J. M. Halls, D. Laird, S. Jia, and S. P. Williams, Adv. Mater. **22**, 3839 (2010).
[3]D. E. Motaung, P. R. Makgwane, and S. S. Ray, Appl. Surf. Sci. **355**, 484 (2015).
[4]W. Zhao, D. Qian, S. Zhang, S. Li, O. Inganäs, F. Gao, and J. Hou, Adv. Mater. **28**, 4734 (2016).
[5]Y. Liang, Z. Xu, J. Xia, S.-T. Tsai, Y. Wu, G. Li, C. Ray, and L. Yu, Adv. Mater. **22**, E135 (2010).
[6]L. J. A. Koster, V. D. Mihailetchi, and P. W. M. Blom, Appl. Phys. Lett. **88**, 93511 (2006).
[7]R. Po, C. Carbonera, A. Bernardi, and N. Camaioni, Energy Environ. Sci. **4**, 285 (2011).
[8]S. H. Park, A. Roy, S. Beaupré, S. Cho, N. Coates, J. S. Moon, D. Moses, M. Leclerc, K. Lee, and A. J. Heeger, Nat. Photonics **3**, 297 (2009).
[9]Y. Zang, X. Gao, X. Lu, Q. Xin, J. Lin, and J. Zhao, Appl. Surf. Sci. **376**, 138 (2016).
[10]M. A. Green, K. Emery, Y. Hishikawa, W. Warta, and E. D. Dunlop, Prog. Photovoltaics **24**, 3 (2016).

[11] J. Kettle, H. Waters, M. Horie, and G. C. Smith, J. Phys. D: Appl. Phys. **49**, 85601 (2016).

[12] X.-Y. Yang, W.-L. Xu, F. Zheng, J.-Q. Liu, and X.-T. Hao, J. Phys. D: Appl. Phys. **49**, 255502 (2016).

[13] S. Oh, I. Jang, S. G. Oh, and S. S. Im, Sol. Energy **114**, 32 (2015).

[14] Y. H. Huh, B. Park, and I. Hwang, J. Appl. Phys. **115**, 124504 (2014).

[15] A. Kumar, S. Sista, and Y. Yang, J. Appl. Phys. **105**, 94512 (2009).

[16] J. C. Wang, X. C. Ren, S. Q. Shi, C. W. Leung, and P. K. L. Chan, Org. Electron. **12**, 880 (2011).

[17] D. Gupta, M. Bag, and K. S. Narayan, Appl. Phys. Lett. **92**, 93301 (2008).

[18] B. Y. Finck and B. J. Schwartz, Appl. Phys. Lett. **103**, 53306 (2013).

[19] J. Wagner, M. Gruber, A. Wilke, Y. Tanaka, K. Topczak, A. Steindamm, U. Hörmann, A. Opitz, Y. Nakayama, H. Ishii, J. Pflaum, N. Koch, and W. Brütting, J. Appl. Phys. **111**, 54509 (2012).

[20] A. Wagenpfahl, D. Rauh, M. Binder, C. Deibel, and V. Dyakonov, Phys. Rev. B **82**, 115306 (2010).

[21] M. Buffière, G. Brammertz, S. Oueslati, H. El Anzeery, J. Bekaert, K. Ben Messaoud, C. Köble, S. Khelifi, M. Meuris, and J. Poortmans, J. Phys. D: Appl. Phys. **47**, 175101 (2014).

[22] W. Tress, A. Petrich, M. Hummert, M. Hein, K. Leo, and M. Riede, Appl. Phys. Lett. **98**, 063301 (2011).

[23] O. J. Sandberg, M. Nyman, and R. Österbacka, Phys. Rev. Appl. **1**, 24003 (2014).

[24] R. A. Street, P. P. Khlyabich, and B. C. Thompson, Org. Electron. **14**, 2932 (2013).

[25] A. Sundqvist, O. J. Sandberg, M. Nyman, J.-H. Smått, and R. Österbacka, Adv. Energy Mater. **6**, 1502265 (2016).

[26] W. Yang, Y. Yao, and C.-Q. Wu, Org. Electron. **14**, 1992 (2013).

[27] V. Amendola, R. Pilot, M. Frasconi, O. M. Maragò, and M. A. Iatì, J. Phys.: Condens. Matter **29**, 203002 (2017).

[28] F. De Castro, A. Laudani, F. R. Fulginei, and A. Salvini, Sol. Energy **135**, 590 (2016).

[29] K. Tada, Org. Electron. **40**, 8 (2017).

[30] M. C. Salvadori, F. S. Teixeira, L. G. Sgubin, W. W. R. Araujo, R. E. Spirin, E. M. Oks, K. M. Yu, and I. G. Brown, Appl. Phys. Lett. **101**, 224104 (2012).

[31] M. C. Salvadori, M. Cattani, F. S. Teixeira, and I. G. Brown, Appl. Phys. Lett. **93**, 073102 (2008).

[32] A. L. Stepanov, D. E. Hole, and P. D. Townsend, J. Non-Cryst. Solids **260**, 65 (1999).

[33] C. Grimaldi, M. Cattani, and M. C. Salvadori, J. Appl. Phys. **117**, 125302 (2015).

[34] W. Möller and W. Eckstein, Nucl. Instrum. Methods Phys. Res., Sect. B **2**, 814 (1984).

[35] W. Möller, W. Eckstein, and J. Biersack, Comput. Phys. Commun. **51**, 355 (1988).

[36] H. Jin, M. Tuomikoski, J. Hiltunen, P. Kopola, A. Maaninen, and F. Pino, J. Phys. Chem. C **113**, 16807 (2009).

[37] M. Glatthaar, M. Riede, N. Keegan, K. Sylvester-Hvid, B. Zimmermann, M. Niggemann, A. Hinsch, and A. Gombert, Sol. Energy Mater. Sol. Cells **91**, 390 (2007).

[38] G. Namkoong, E. M. Younes, T. M. Abdel-Fattah, E. M. El-Maghraby, A. H. Elsayed, and A. H. Abo Elazm, Org. Electron. **25**, 237 (2015).

[39] A. Gusain, S. Singh, A. K. Chauhan, V. Saxena, P. Jha, P. Veerender, A. Singh, P. V. Varde, S. Basu, D. K. Aswal, and S. K. Gupta, Chem. Phys. Lett. **646**, 6 (2016).

[40] F. A. de Castro, J. Heier, F. Nüesch, and R. Hany, IEEE J. Sel. Top. Quantum Electron. **16**, 1690 (2010).

[41] B. Romero, G. del Pozo, and B. Arredondo, Sol. Energy **86**, 3026 (2012).

[42] M. Carrara, J. J. Kakkassery, J.-P. Abid, and D. J. Fermín, ChemPhysChem **5**, 571 (2004).